Local Deposition of Polypyrrole on Aluminum by Anodizing, Laser Irradiation, and Electrolytic Polymerization and Its Application to the Fabrication of Micro-actuators.

Y. Akiyama, T. Kikuchi*, M. Ueda, M. Iida, M. Sakairi and [1]H. Takahashi

Graduate School of Engineering, Hokkaido University

N13, W8, Kita-Ku, Sapporo, Japan

Corresponding author: T. Kikuchi

TEL: +81-11-706-7112

FAX: +81-11-706-7881

e-mail: kiku@elechem1-mc.eng.hokudai.ac.jp

[1] ISE member

Abstract

Polypyrrole was deposited at selected areas on aluminum by anodizing, laser irradiation, and electrolytic polymerization, and the application of the technique for fabricating micro-actuators was attempted. Aluminum specimens covered with porous type anodic oxide films were irradiated with a pulsed Nd-YAG laser to remove the

oxide films locally, and then thin Ni layers were deposited at areas where film had been removed. Polypyrrole could be successfully deposited only on the Ni layer by anodic polarization of the specimens in pyrrole monomer solution, and a polypyrrole / Ni bilayer-structure could be obtained by dissolution of the aluminum substrate and anodic oxide film in NaOH solutions. The bilayer structure was found to be inactive to doping and dedoping of ions during anodic and cathodic polarization. A three layer structure, nitrocellulose / Ni / polypyrrole, fabricated by electrolytic polymerization after nitrocellulose coating on a Ni layer detached from the aluminum substrate, showed ion-doping and –dedoping activity, suggesting the possibility of fabricating micro-actuators in this manner.

Key words: aluminum, anodizing, conducting polymer, electrolytic polymerization, micro-actuator

1. INTRODUCTION

The authors have been developing a novel method of micro-patterning of

aluminum using anodizing, laser irradiation, and electrochemical techniques [1-8]. In the process, aluminum specimens covered with anodic oxide films are irradiated with a pulsed Nd-YAG laser to remove the oxide film locally [1], and then a metal layer is deposited by electroplating [2,3] or electroless plating [4-6] at areas where oxide films have been removed by laser irradiation. An acrylic acid resin was also deposited locally by electrophoretic deposition after laser irradiation [7]. Local etching and anodizing / dissolution after laser irradiation enabled the formation of micro-pores and –grooves on the aluminum substrate [8]. The authors have recently applied these techniques to the fabrication of printed circuit boards [9,10], plastic injection molds [11], micro-reactors [12], and three-dimensional micro-structures [13].

In the fabrication process of the three-dimensional microstructures [13], cylindrical and prismatic aluminum bars covered with anodic oxide film were rotated and moved up- and down-wards during laser irradiation, and later metals and acrylic acid resins were deposited electrochemically. After the metal / acrylic acid resin deposition, the specimens were immersed in a NaOH solution to lift off the metal- or organic-layer by dissolution of the aluminum substrate and anodic oxide film.

Free-standing metal / acrylic acid resin structures of cylindrical and prismatic network cages, rings, springs, and bellows were obtained by these processes.

The success of the fabrication of free-standing 3D micro-structures suggested the authors to deposit conducting polymers locally on these, and to fabricate micro-actuators by a combination of the techniques described above with electrolytic polymerization of pyrrole [14]. Actuators based on conducting polymers, such as polypyrrole (PPy), polyaniline, polythiophene, polymethylaniline, poly(3-methylthiophene), poly(i-methylpyrrole), and polyulethane have been investigated extensively [15-25] for the fabrication of micro-electromechanical systems (MEMS) and bio-mimetic devices, and among these actuators polypyrrole-based actuators appear to be the most attractive, due to the high electro-conductivity and high stability in various media [15]. The principle of actuators consisting of a bilayer structure of a conducting polymer / non-conducting organic layer (or metal layer), is based on the volume expansion of the conducting polymer by ion-doping into the polymer film and volume shrinkage by ion-dedoping into electrolyte solutions. The expansion and shrinkage of the polymer enable the swing of the bilayer actuators by

changing applied potential, since the backing layer does not change in volume. Micrometer scale actuators are fabricated preferentially by photolithography with a resist pattern formation and selective polymerization. As photolithography is seldom applied to materials with three-dimensional (3D) structures such as rods, spheres, and others, a technique to fabricate 3D micro-actuators without photolithography would be useful.

The present investigation used a micro-patterning technique in the fabrication of PPy micro-actuators by aluminum anodizing, laser irradiation, and pyrrole electrolytic polymerization.

2. EXPERIMENTAL

2.1 Specimens and anodizing

Highly pure aluminum plate (99.99 wt%, 0.35 mm thick, 20 x 18 mm with a handle, Nippon Light Metal) was used as the specimens. The specimens were degreased ultrasonically in C_2H_5OH for 10 min, and then electropolished in 13.6 M CH_3COOH / 2.56 M $HClO_4$ solution at 28 V and 280 K. After electropolishing, the

specimens were anodized in 0.22 M $(COOH)_2$ solution at 293 K for 30 min with a constant current of 100 Am^{-2} to form 9 μm thick porous type oxide films. The anodized specimens were immersed in 0.029 M alizarin red S dying solution at 323 K for 5 min, and then boiled in doubly distilled water for 15 min to seal the pores.

2.2 Laser irradiation and local Ni plating

Two kinds of Ni^{2+} ion solution were prepared for laser irradiation and Ni electroplating. Solution-I was composed of 0.31 M $NiSO_4$ and 0.40 M H_3BO_3, and Solution-II of 1.0 M $NiSO_4$, 0.5 M H_3BO_3, 0.2 M $NiCl_2$, and additives of saccharin sodium and 2-butyne-1, 4-diol (see Table 1).

Specimens were immersed in Ni^{2+} solutions in a cell, and set in a defocused position 5 mm from the focal plane of a laser beam that had passed through a beam splitter, a pentagonal-shaped iris diaphragm, a convex lens with 60 mm focal length, and a quartz window. Details of the laser irradiation setup have been shown elsewhere [7]. The set specimens were irradiated with 10 mW of a pulsed Nd-YAG laser (GCR-130-10, Spectra Physics) to remove the anodic oxide film. The laser used the second harmonic wave with 532 nm wavelength, 8 ns pulse width, 10 Hz frequency, and

< 0.5 mrad beam divergence (full angle). During the laser irradiation, the specimen was moved at 200 μm/s with a PC-controlled XY-stage to obtain square and mesh patterned laser-irradiated areas.

The laser-irradiated specimens were polarized cathodically for 10 - 20 min at constant potentials between –1.0 - -1.1 V and 293 K in the Ni^{2+} solutions which had been used for the laser irradiation [2]. A Pt plate was used as the counter electrode and a saturated KCl-Ag/AgCl electrode as the reference electrode for the Ni electroplating.

2.3 Fabrication of the bilayer structure of polypyrrole / Ni layers

The bilayer structure of polypyrrole and Ni layers was fabricated through two processes (Fig. 1). In Process-A, electrolytic polymerization was carried out before separating the bilayer structure from the aluminum specimen, while, in Process-B, polypyrrole was deposited on the Ni layer after lifting it off the aluminum specimen.

In Process-A, the Ni-deposited aluminum specimen was set in de-aerated 0.1 M HNO_3 / 0.2 M pyrrole solution at room temperature, and anodically polarized for 10 - 120 min at 0.55 - 0.65 V (vs. Ag/AgCl) to deposit PPy films on the Ni metal layer. Structural changes in the specimens by electrolytic polymerization were examined by

confocal scanning laser microscopy (CSLM: 1SA21, LASERTEC). For the observations of the vertical cross sections of specimens, they were embedded in epoxy resin and polished mechanically. Finally, the specimens were immersed in 3 M NaOH solution at room temperature for 30 min to dissolve the aluminum substrate and oxide films. The fabrication process of the PPy / Ni bilayer microstructure is shown in Fig. 1 (Process-A).

In process-B, Ni-deposited aluminum specimens were immersed in 3 M NaOH at room temperature for 30 min to dissolve the aluminum substrate and oxide films. One surface of the Ni metal layer obtained in this manner was covered with a nitrocellulose film by painting one surface of the specimen with a nitrocellulose / ethyl acetate solution with a brush. The Ni metal film, one side of which had been shielded with nitrocellulose, was polarized anodically in 0.1 M sodium dodecylbenzensulfate (NaDBS) / 0.2 M pyrrole solution at room temperature for 120 min at 0.60 V (vs. Ag/AgCl) to obtain PPy films on the uncovered Ni metal layer side (see Fig. 1, Process-B).

Cyclic voltammograms of the two- and three-layer structures obtained by

process-A and –B were measured in 0.1 M NaDBS solution, at a potential scanning rate of 5 mV/s between 0.4 and -0.8 V (vs. Ag/AgCl), and the motion of the microstructures was recorded on video during the cyclic voltammetry.

3. RESULTS AND DISCUSSION

3.1 Deposition of PPy on the Ni-deposited layer

Figure 2 shows the anodic polarization curve, the i_a vs. E curve, obtained at a 2 mV / s scanning rate in 0.1 M HNO_3 / 0.2 M pyrrole solution at room temperature on the aluminum specimen after anodizing, laser irradiation, and Ni electroplating. Here, the specimen was irradiated with the laser to obtain a 3 x 3 mm^2 film removed area, and then this area was covered with a Ni metal layer by cathodic polarization in Solution-I. The i_a value shows a peak at E = 0.10 V, and very small values at E = 0.30 – 0.55 V. The i_a peak of at 0.10 V corresponds to active dissolution of Ni metal, while the small current between 0.30 V and 0.55 V corresponds to the passive current on Ni. At potentials above E = 0.55 V, the i_a rapidly increases at more positive potentials, accompanied by changes in color from gray to black at the Ni-deposited area,

suggesting the deposition of PPy. In the E_a > 0.55 V region, PPy is deposited electrochemically on the Ni layer according to the following reaction.

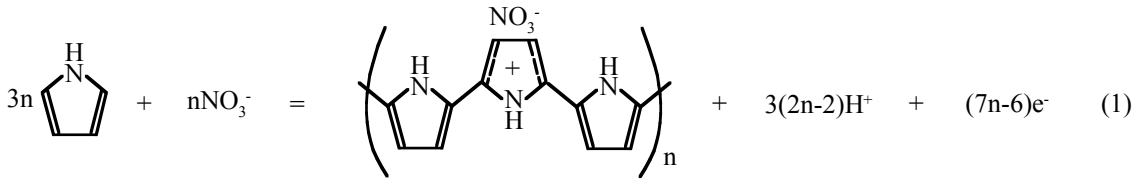

During the electrolytic polymerization of pyrrole, NO_3^- ions are considered to become doped into the PPy film.

Figure 3 shows CSLM two-dimensional contrast images of the surface of Ni layers polarized at a) E_a = 0.55, b) 0.60, and c) 0.65 V for t_a = 15 to 20 min in 0.1 M HNO_3 / 0.2 M pyrrole solution. At E_a = 0.55 (Fig. 3-a) and 0.6 V (Fig. 3-b), the whole Ni layer surface is uniformly covered with black, adhesive PPy film, and the surface of the PPy films becomes rougher at higher potentials. However, at E_a = 0.65 V, the PPy film is removed locally from the Ni metal layer after drying the specimens, due to poor adhesion.

Figure 4 shows a CSLM contrast image of the cross-section of a specimen at the laser-irradiated area after polarization at E_a = 0.60 V for 30 min in 0.1 M HNO_3 / 0.2 M pyrrole solution. The CSLM image shows a four layer structure: aluminum substrate,

Ni-deposited layer, PPy layer, and epoxy resin. The PPy layer / epoxy resin and Al /Ni layer interfaces are traced with white and black lines to show their boundaries. It can be seen from Fig. 4 that the interface between aluminum substrate and Ni metal layer is relatively rough due to laser ablation of the aluminum substrate during laser irradiation, and that, on the aluminum, there is a 14 μm-thick Ni layer with a surface roughness similar to that at the Al / Ni interface. Figure 4 also shows that an about 30 μm-thick PPy layer is deposited on the Ni layer, and that the surface roughness of the PPy layer is much higher than that of the Ni layer.

Figure 5 shows the changes in the thickness of the PPy layer, δ, with polarization time, t_a, at E_a = 0.60 V in 0.1 M HNO_3 / 0.2 M pyrrole solution. The δ increases rapidly in the initial period, and then increases linearly with t_a at a rate of about 40 μm / h.

Figure 6-a shows a photograph of the PPy micro-pattern fabricated on the aluminum specimen by anodizing, laser irradiation, Ni electroplating, and PPy deposition. In Fig. 6-a, the black parts correspond to the PPy-deposited area, and the gray parts to the anodic oxide film-covered area not subjected to laser irradiation. The

PPy microstructure consists of a mesh-pattern with 120 μm line width in a 9 x 3 mm rectangular pattern. As can be seen from Fig. 6-a, PPy is deposited only at the laser-irradiated area, clearly suggesting that the anodic oxide films are very stable during the Ni plating and PPy deposition, and that they can be used as templates.

Fig. 6-b shows a photograph of the PPy / Ni bilayer microstructure after immersing the PPy-patterned specimen (see Fig. 6-a) in 3 M NaOH solution. Fig. 6-b clearly shows that the PPy / Ni bilayer structure can be detached from the specimen.

3.2 Cyclic voltammograms

Figure 7 shows the cyclic voltammogram at the scanning rate of 5 mV/s in 0.1 M NaDBS solution at room temperature on a PPy / Ni bilayer ribbon structure (0.3 x 12 mm) fabricated by Process-A (see Fig. 1 b)). The electrolytic polymerization for the formation of PPy layer was carried out at E_a = 0.60 V in 0.1 M HNO_3 / 0.2 M pyrrole solution. The anodic current, i, increases by scanning the potential in the anodic direction from E = 0 V with E up to E = 0.3 V, and, during the potential scanning in the cathodic direction from 0.3 V i decreases, and changes to cathodic current at

about 0 V, showing an increase in the cathodic current with E down to - 0.8 V. The potential scanning in the anodic direction from E = -0.8 V causes a decrease in the cathodic current, passing zero at –0.2 V becoming an anodic current. As shown in Fig. 7, the PPy / Ni bilayer structures fabricated by Process-A shows some hysteresis in the cyclic voltammogram, suggesting an electro-inactive state of polypyrrole with only little doping and de-doping of ions taking place during the potential scanning between 0.3 and –0.8 V. The motion of the ribbon structure was examined on video, but no motion could be detected during the potential scanning.

The cyclic voltammogram of the PPy-deposited specimen before removal from the Al substrate showed an anodic peak and a cathodic peak (not shown here), and the electro-inactive state of the PPy / Ni bilayer structures fabricated by Process-A is considered to be due to the immersion in NaOH solution. Osaka et al. [26-29] reported that electro-inactive PPy can be obtained by electrolytic polymerization in an aqueous alkaline solution. Inganas et al. [30] found that the conductance of PPy films decrease drastically after immersion in alkaline solution. Kuwabata [31] reported that the transition of PPy from an electro-active state to an electro-inactive state is due to the

disruption of N-H bonds in PPy in alkaline solution. Xie et al. [32] examined the transition of polypyrrole by in situ FTIR spectroscopy, and found that some pentacyclic rings in the PPy chain are opened up after long periods of immersion in alkaline solutions.

The transient of PPy to an electro-inactive state during immersion of PPy-deposited aluminum specimens in NaOH solution observed in this investigation can be considered to be due to the influence of OH^- ions, as reported by the authors above. De-protonation of PPy by PPy-reduction may be an additional reason as will be detailed in the following:

When PPy-deposited specimens were immersed in NaOH solution, the aluminum substrate dissolves according to the following equations:

$$Al + 4OH^- = [Al(OH)_4]^- + 3e- \quad (2)$$

$$3H_2O + 3e- = 3OH^- + (3 / 2)H_2 \quad (3)$$

Equation 2 is the anodic dissolution of aluminum and Eq. 3 is the cathodic reduction of water to evolve H_2. The overall reaction of the aluminum substrate dissolution can be expressed in the following equation.

$$Al + 3H_2O + OH^- = [Al(OH)_4]^- + (3/2)H_2 \qquad (4)$$

The counter reaction to Eq. 2 could also be a reduction of PPy, leading to de-doping of NO_3^- ions.

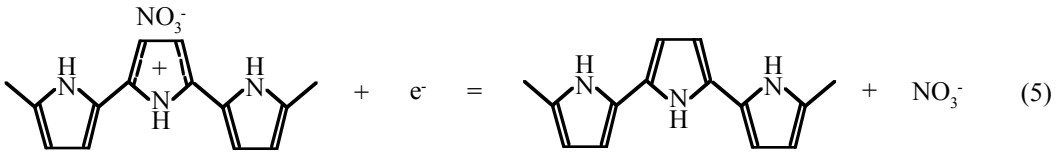

(5)

Figure 8 shows the cyclic voltammogram at a scanning rate of 5 mV/s in 0.1 M NaDBS solution at room temperature for a PPy/Ni/nitrocellulose three-layer microstructure fabricated by process-B (see Fig. 1)). There is an oxidation peak at approximately -0.25 V and a reduction peak around -0.60 V. These peaks correspond to electrochemical doping / dedoping of solvated Na^+ ions, $(Na^+)_s$, into the PPy film.

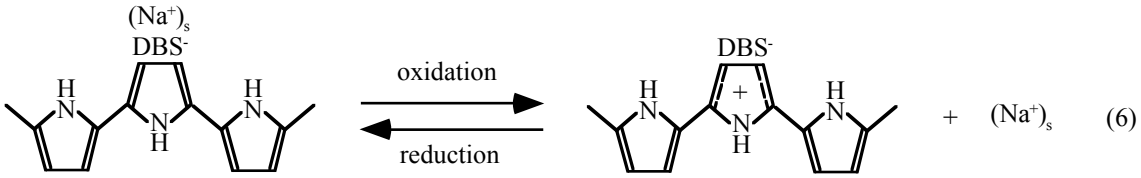

(6)

The PPy formed by Process-B are doped with DBS^- ions, because electrolytic polymerization of pyrrole has been carried out in NaDBS solution. The relatively large size of DBS^- ions causes the doping / de-doping of $(Na^+)_s$, rather than that of DBS^- during the cyclic voltammogram measurements. It can be seen from Fig. 8 that the nitrocellulose / Ni / PPy three-layer structure fabricated by Process-B has electro-active

properties. This is due to the electrolytic polymerization occurring after removing the Ni layer from the aluminum specimen. It is noteworthy that the current density of the cyclic voltammogram in the electro-active state is much higher than that in the electro-inactive state (comparing Figs. 7 and 8).

Fig. 9 shows photographs illustrating the movement of the PPy/Ni/ nitrocellulose microstructure by switching the applied potential from a) -0.6 V to b) 0.6 V in 0.1 M NaDBS solution. The microstructure was a 2 x 14 mm ribbon connected to Cu wire with Dotite electro-conductive paste. Figure 9-a shows the vertical cross section of the three layer-structure: a PPy layer (left), a Ni layer (middle), and a nitrocellulose layer (right). At E = -0.6 V, the ribbon appears like a plain sheet, forming a thin straight line, while at E = 0.6 V the ribbon bends upwards and twists clock wise. The potential change from 0.6 V to – 0.6 V returned the ribbon to the same shape as in Fig. 9-a. This strongly suggests that anodic polarization of the microstructure causes the volume of PPy to shrink, leading to the bending and twisting of the microstructure.

The motion induced by the potential switching from –0.6 V to 0.6 V was 5 times faster than that from 0.6 V to –0.6 V. This is due to the relatively high conductivity of

PPy at –0.6 V and the decrease in the conductivity with de-doping $(Na^+)_s$.

The present investigation showed the fabrication of an actuator consisting of a PPy / Ni / Nitrocellulose three layer structure, by successive processes of aluminum anodizing, laser irradiation, Ni electroplating, substrate dissolution, and pyrrole electrolytic polymerization. This result indicates the feasibility of fabricating micro-manipulators by applying the technique described here to the three dimensional microstructures which have been developed in previous work.

4. CONCLUSIONS

The following conclusions may be drawn.

1. Poly-pyrrole (PPy) can be deposited successfully at selected areas of aluminum by anodizing, laser irradiation, Ni electroplating, and electrolytic polymerization, to form PPy micro patterns.

2. Micro-structures consisting of PPy / Ni bilayers can be fabricated by immersing PPy-deposited specimens in NaOH. Poly-pyrrole becomes electro-inactive during immersion in NaOH, due to a reaction of PPy with OH^- ions.

3. The PPy / Ni / Nitrocellulose three-layer structure can be fabricated by anodizing, laser irradiation, Ni electroplating, Ni-film detachment, nitrocellulose coating, and PPy electrolytic polymerization. The PPy in the three-layer structure fabricated in this manner is electro-active, and shows an oxidation current peak at –0.25 V and a reduction current peak at –0.60 V in the cyclic voltammogram. A ribbon shaped PPy / Ni / nitrocellulose structure moves reversibly by changing the potential from -0.6 to 0.6 V, and vice versa.

References

1) H. Takahashi, K. Nukui, M. Seo, Y. Matsumi, and M. Kawasaki, Proc. of Symp. on Oxide Films on Metals and Alloys VII, Sponsored by Electrochem. Soc. (1995) 50.

2) M. Sakairi, J. Wakabayashi, H. Takahashi, N. Katayama, J. Surface Finishing. Soc. Jpn. 49 (1998) 1220.

3) M. Sakairi, Z. Kato, S. Z. Chu, H. Takahash, Y. Abe, and N. Katayama, Electrochemistry 71 (2003) 920.

4) S. Z. Chu, M. Sakairi, H. Takahashi, and Z. X. Qui, J. Electrochem Soc. 146 (1999)

537.

5) S.Z. Chu, M. Sakairi, and H. Takahashi, J. Electrochem. Soc. 146 (1999) 2876.

6) S. Z. Chu, M. Sakairi, H. Takahashi, K. Shimizu, and Y. Abe, J. Electrochem. Soc. 147 (2000) 2182.

7) T. Kikuchi, S. Z. Chu, S. Jonishi, M. Sakairi, and H. Takahashi, Electrochim. Acta 47 (2001) 225.

8) T. Kikuchi, M. Sakairi, H. Takahashi, Y. Abe and N. Katayama , J. Electrochem. Soc. 148 (2001) C740.

9) H. Takahashi, M. sakairi, and T. Kikuchi, J. Surface Sci. Soc. Jpn. 22 (2001) 370

10) T. Kikuchi, M. Sakairi, H. Takahashi, Y. Abe, and N. Katayama, J. Surface Finishing Soc. Jpn. 54 (2003) 137.

11) S. M. Moon, M. Sakairi, H. Takahashi and K. Shimamura, Elecrtrochemisty 71 (2003) 260.

12) H. Takahashi, M. Sakairi, K. Watanabe, T. Kikuchi, and M. Yamada, J. Surface finishing soc. Jpn. 54 (2003) 436.

13) T. Kikuchi, M. Sakairi, and H. Takahashi, J. Electrochem. Soc. 150 (2003) C567

14) Y. Akiyama, T. Kikuchi, M. Iida, M. Ueda, M. Sakairi, and H. Takahashi, Abstract of 110th Meeting of Surf. Fin. Soc. Jpn. (2004) 150.

15) T. F. Otero, H. Grande, and J. Rodriguez, Syn. Metals 83 (1996) 205.

16) T. F. Otero and J. M. Sansinena, Advanced Mate. 10 (1998) 491.

17) T. F. Otero, I. Cantero, and H. Grande, Elechtrochim. Acta 44 (1999) 2053.

18) T. F. Otero and I. Boyano, J. Phys. Chem. B107 (2003) 6730.

19) J. W. Paquette, K. J. Kim, D. Kim, Sensors and Actuators A118 (2005) 135.

20) J. H. Lee, J. H. Lee, J. D. Nam, H. Choi, K. Jung, J. W. Jeon, Y. K. Lee, K. J. Kim, and Y. Tak, Sensors and Actuators A118 (2005) 98.

21) M. Onoda, H. Shonaka, and K. Tada, Current Appl. Phys. 5 (2005) 194.

22) W. Lu, I. D. Norris, and B. R. Mattes, Austr. J. Chem. 58 (2005) 263.

23) M. A. Careem, K. P. Vidanapathirana, S. Shaarup, K. West, Solid State Ionics 175 (2004) 725.

24) S. Hara, T. Zama, W. Takashima, and K. Kaneto, Synthetic Metals 149 (2004) 199.

25) T. Zama, S. Hara, W. Takashima, and K. Kaneto, Bull. Chem. Soc. Jpn. 78 (2005) 506.

26) T. Osaka, K. Ouchi and T. fukuda, Chem. Lett. (1990) 1535.

27) T. Osaka, T. Fukuda, K. Ouchi, T. Nakajima, Denki Kagaku 59 (1991) 1019.

28) T. Osaka, T. Momma, and H. Kanagawa, Chem. Lett., (1993) 649.

29) T. Osaka, T. Momma, S. Komaba, and H. Kanagawa, J. Electroanal. Chem. 372 (1994) 201.

30) O. Inganas, R. Erlandsson, c. Nylander and I. Lundstrom, J. Phys. Chem. Solids 45 (1984) 432.

31) S. Kuwabata, N. Nakamura, and H. Yoneyama, J. Electrochem. Soc. 137 (1990) 2147.

32) H. Xie, M. Yan, and Z. Jiang, Electrochim. Acta 42 (1997) 2361.

Captions

Table. 1 The compositions Ni electroplating solutions and operating conditions.

Fig. 1 Fabrication of PPy microstructures by anodizing, laser irradiation, Ni / PPy electrodeposition, and dissolution of the aluminum substrate and oxide films.

Fig. 2 Change in anodic current density, i_a, with potential, E, in 0.1 M HNO_3 / 0.2 M pyrrole solution using Ni electrodeposited specimens after anodizing, laser irradiation, and Ni electroplating.

Fig. 3 CSLM contrast images of the surface of specimens after laser irradiation, Ni electroplating, and electro-polymerization for a) E_a = 0.55 V, b) 0.60 V, and c) 0.65 V.

Fig. 4 CSLM contrast image of a vertical cross-section of a specimen at an area with deposited PPy.

Fig. 5 Change in the PPy film thickness, δ, with electro-polymerization time, t_a, in 0.1 M HNO_3 / 0.2 M pyrrole solution.

Fig. 6 Optical micrograph of a) PPy micro-pattern on an aluminum specimen after anodizing, laser irradiation, Ni electroplating, and PPy electro-polymerization, and b) PPy / Ni bilayer microstructure after dissolution of the aluminum substrate and oxide

films.

Fig. 7 Cyclic voltammogram of the PPy / Ni microstructure in 0.1 M NaDBS solution. The microstructure was fabricated by process-A.

Fig. 8 Cyclic voltammogram of the PPy / Ni / Nitrocellulose microstructure in 0.1 M NaDBS solution. The microstructure was fabricated by process-B.

Fig. 9 Video images of the bending behavior of the PPy / Ni / Nitrocellulose microstructures in 0.1 M NaDBS solution at applied potentials of a) -0.6 V and b) 0.6 V.

Table. 1

The compositions and operating conditions of Ni electroplating.

Composition / Codition	Solution I	Solution II
$NiSO_4$	0.31 M	1.0 M
H_3BO_3	0.40 M	0.50 M
$NiCl_2$	-	0.20 M
Saccharin sodium	-	0.01 M
2-Butyne-1,4-diol	-	0.0025 M
pH	3.40	2.06
Temperature	293 K	293K
Potential (vs. sat. Ag/AgCl)	-1.1 V	-1.0 V
Plating time	20 min	10 min

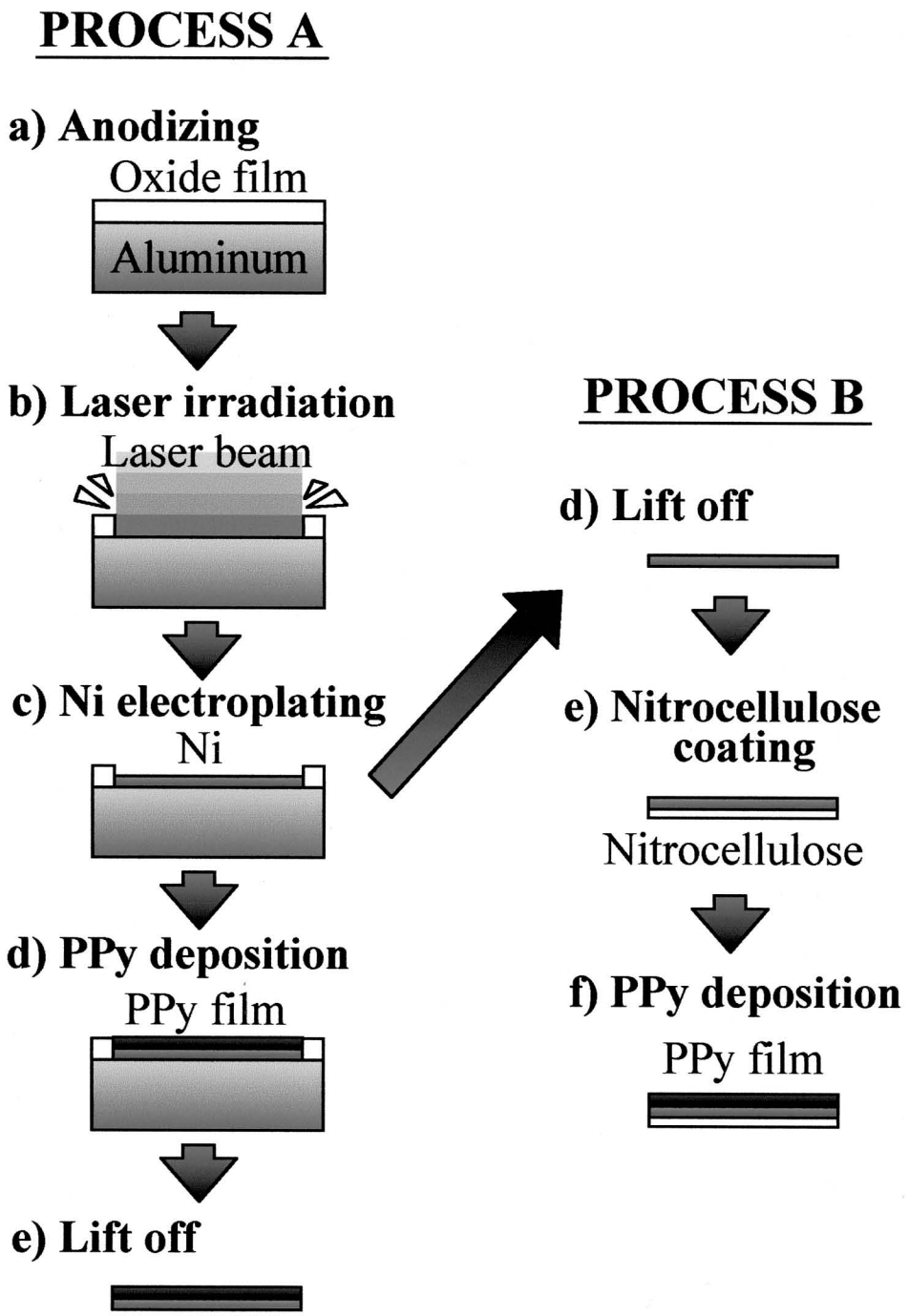
PROCESS A
a) Anodizing
Oxide film
Aluminum
b) Laser irradiation
Laser beam
c) Ni electroplating
Ni
d) PPy deposition
PPy film
e) Lift off
PROCESS B
d) Lift off
e) Nitrocellulose coating
Nitrocellulose
f) PPy deposition
PPy film

Fig. 1

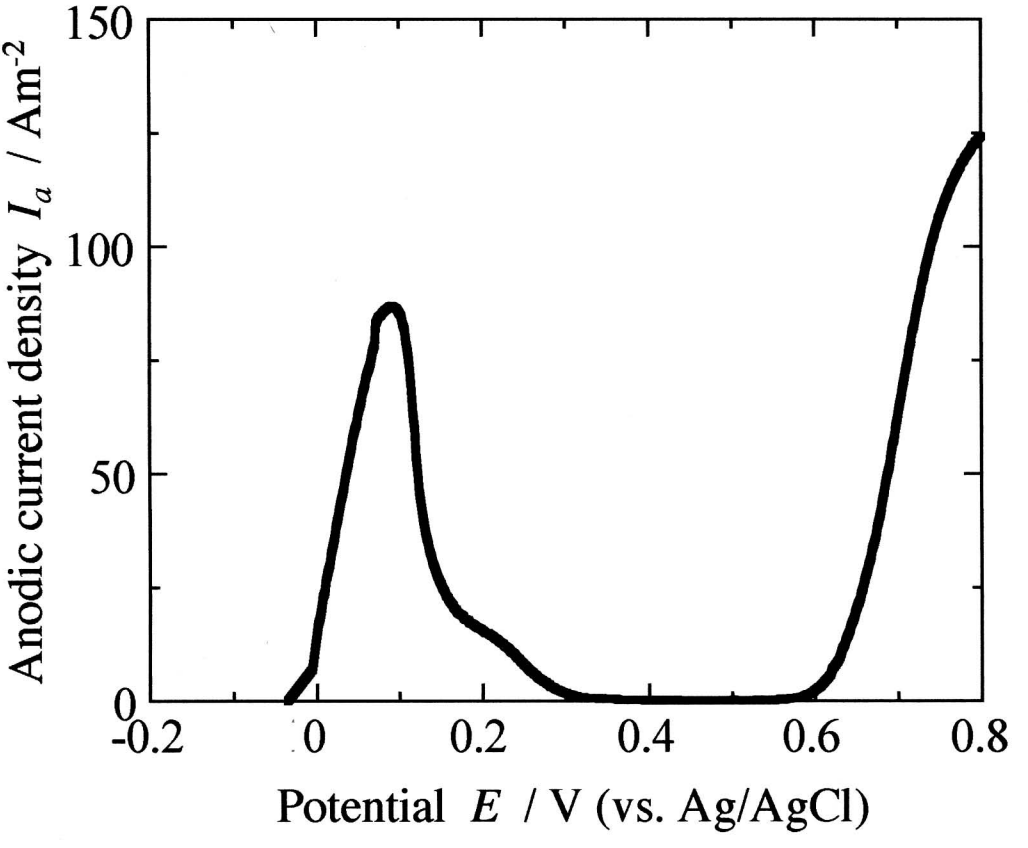
150
100
50
0
-0.2
0
0.2
0.4
0.6
0.8
Anodic current density I_a / Am^{-2}
Potential E / V (vs. Ag/AgCl)

Fig. 2

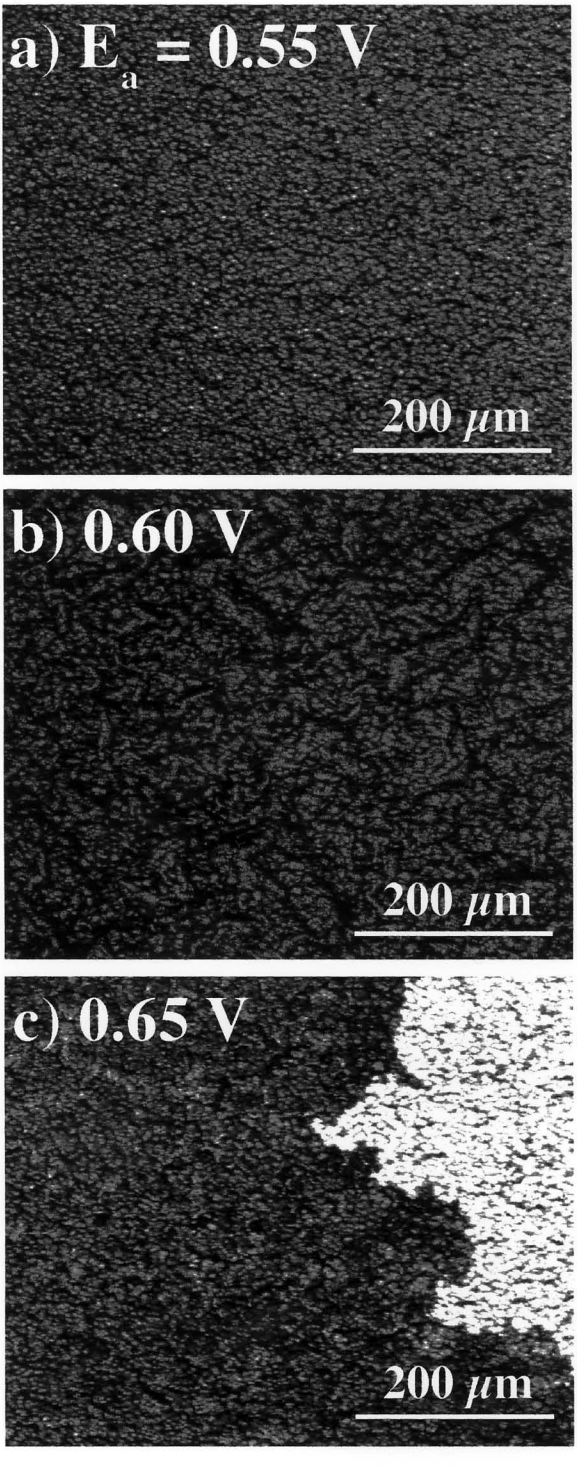

Fig. 3

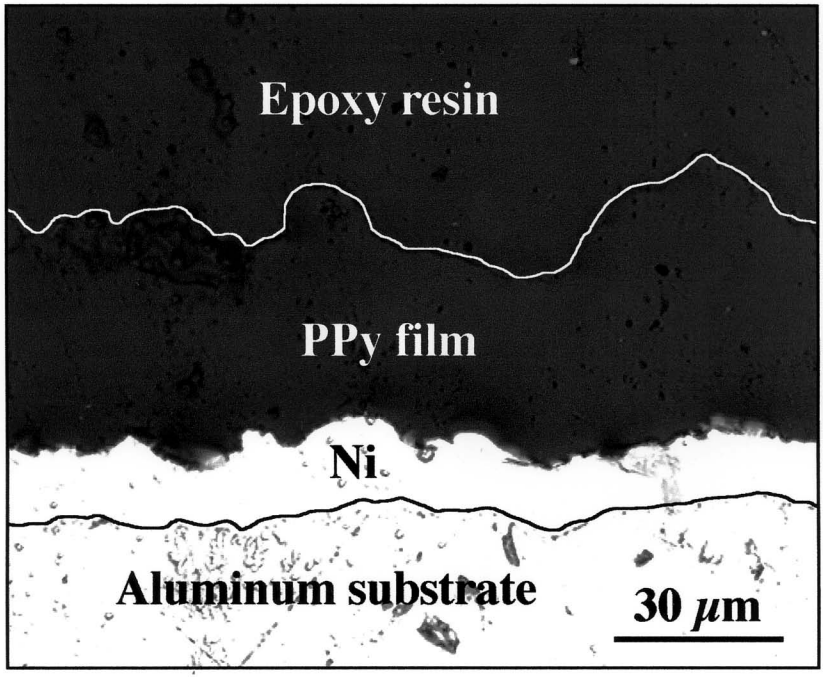

Fig. 4

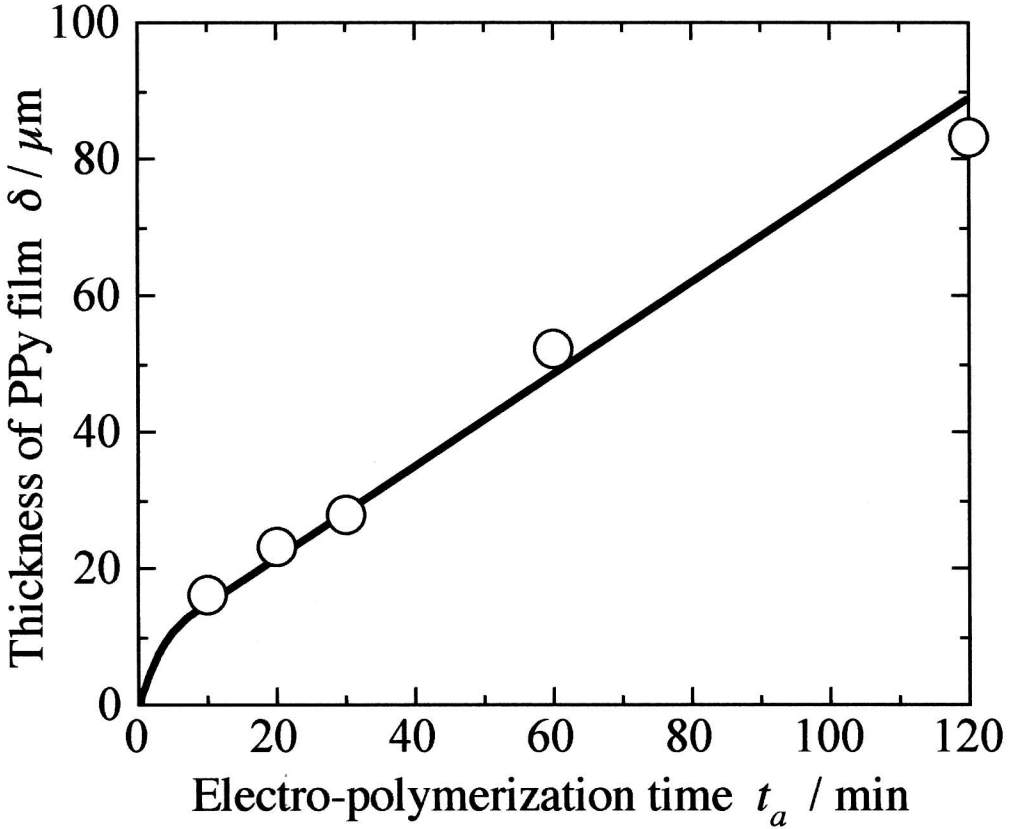
100
80
60
40
20
0
Thickness of PPy film δ / μm
0
20
40
60
80
100
120
Electro-polymerization time t_a / min

Fig. 5

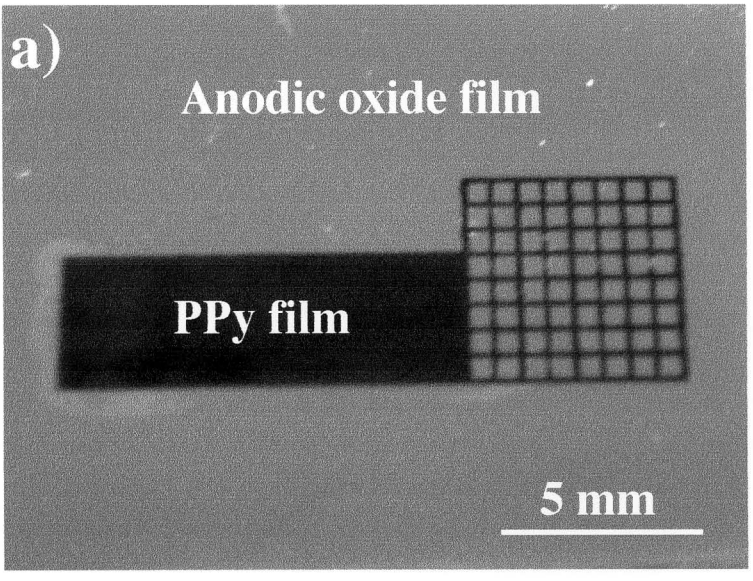

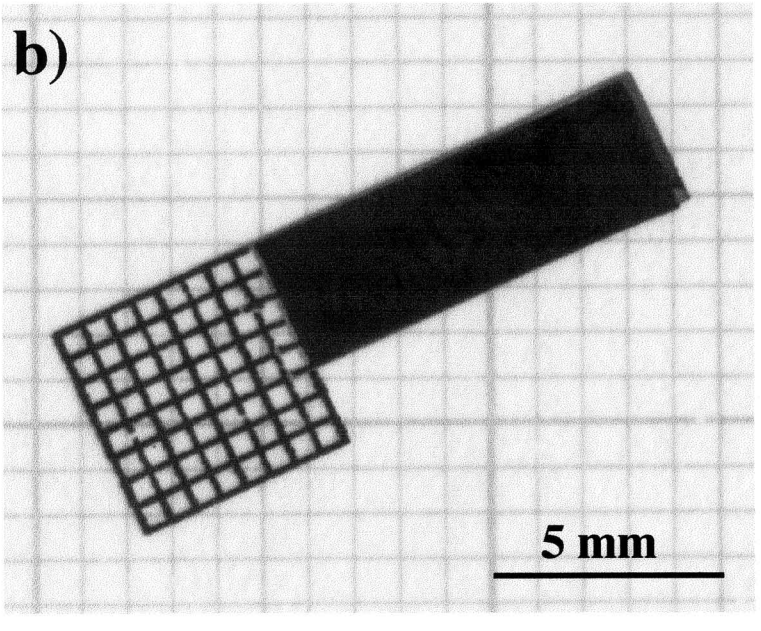

Fig. 6

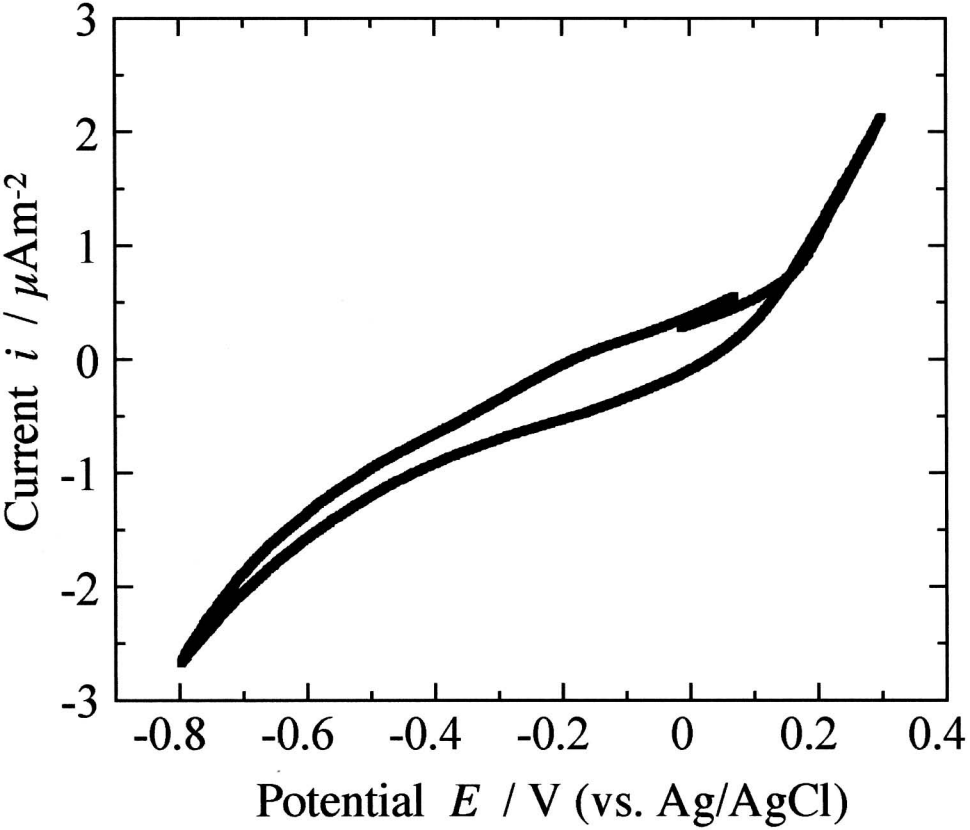
3
2
1
0
-1
-2
-3
Current i / μAm^{-2}
-0.8
-0.6
-0.4
-0.2
0
0.2
0.4
Potential E / V (vs. Ag/AgCl)

Fig. 7

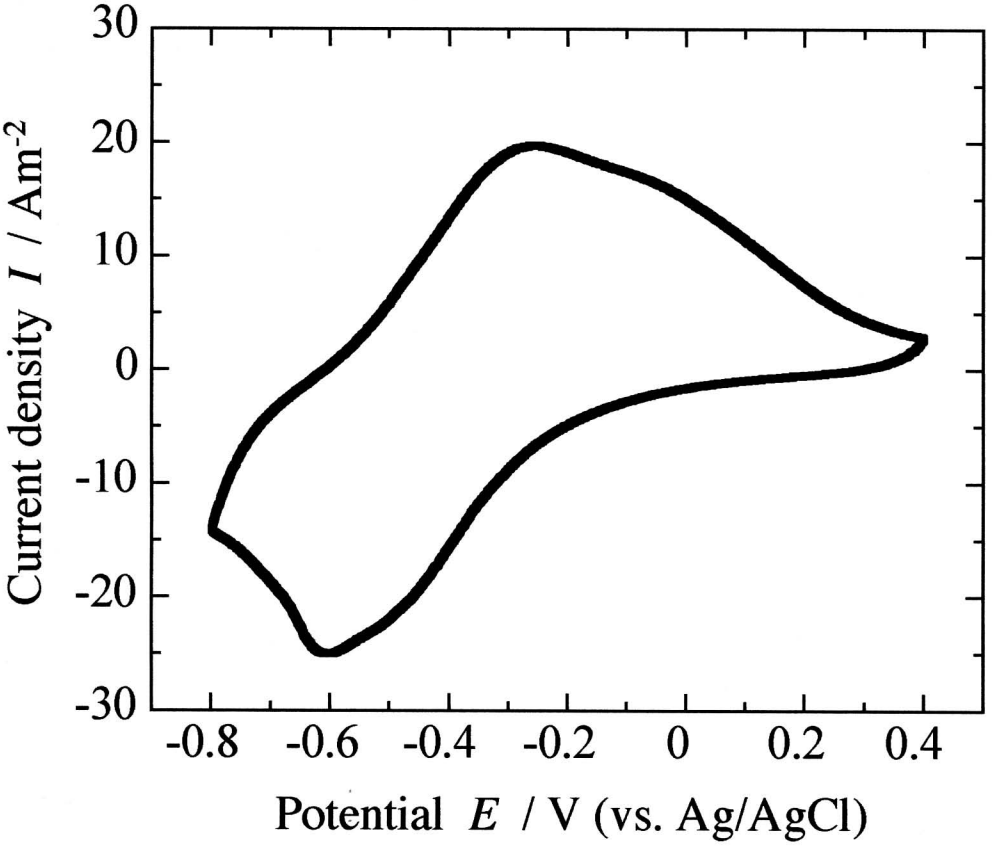
30
20
10
0
-10
-20
-30
Current density I / Am^{-2}
-0.8
-0.6
-0.4
-0.2
0
0.2
0.4
Potential E / V (vs. Ag/AgCl)

Fig. 8

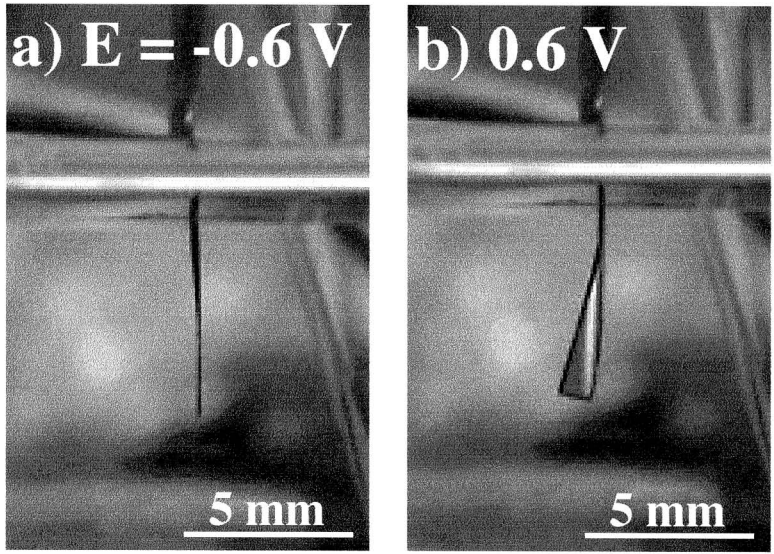

Fig. 9

Y. Akiyama, T. Kikuchi, M. Ueda, M. Iida, M. Sakairi and H. Takahashi